Supplemental Figure 1

A

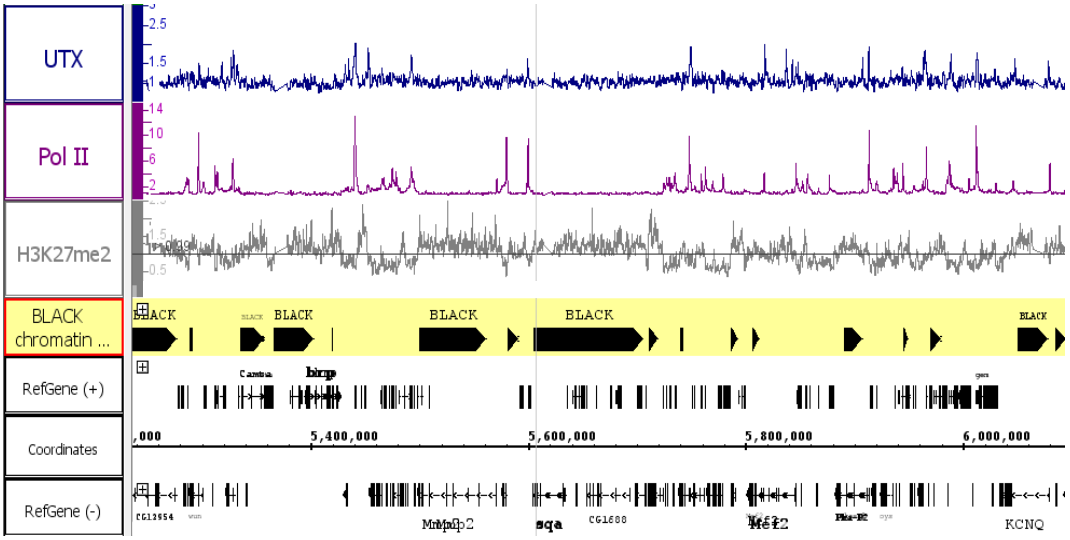

B

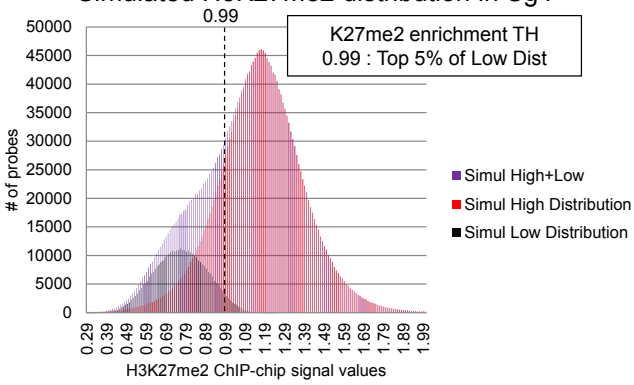

C

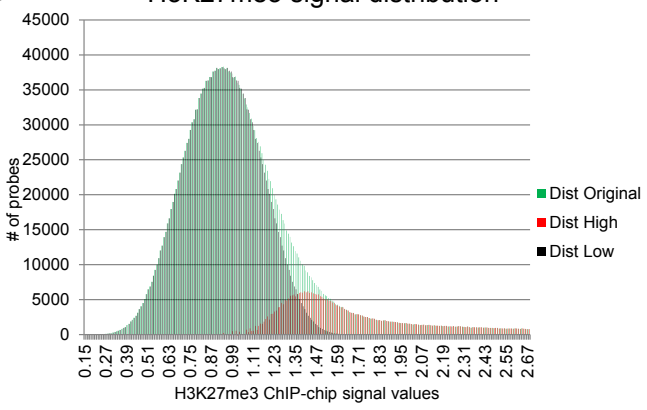

D

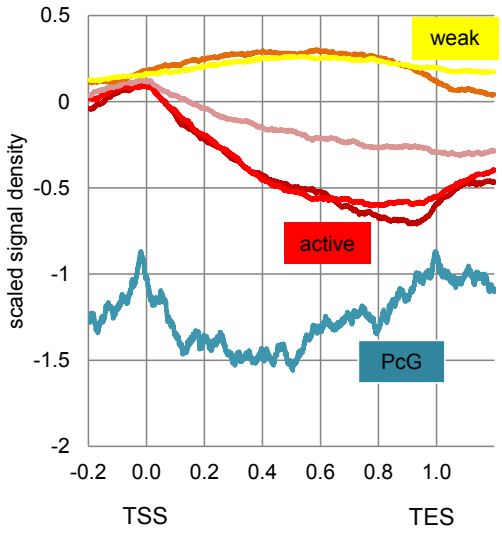

E

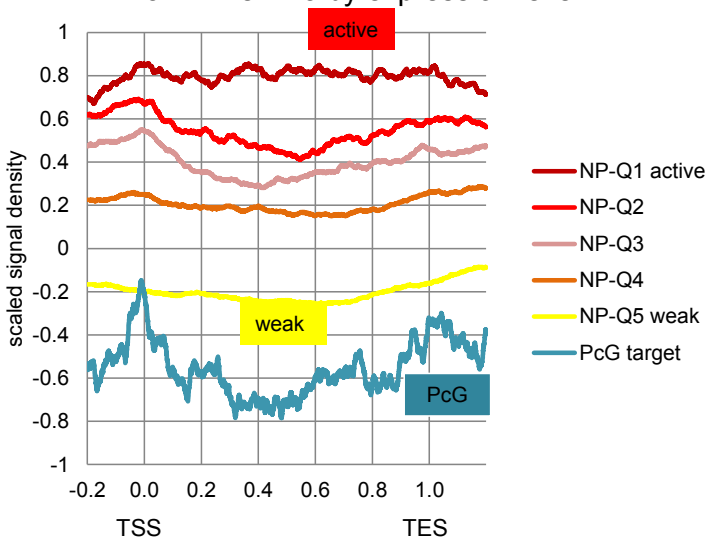

Supplemental Figure 2

A

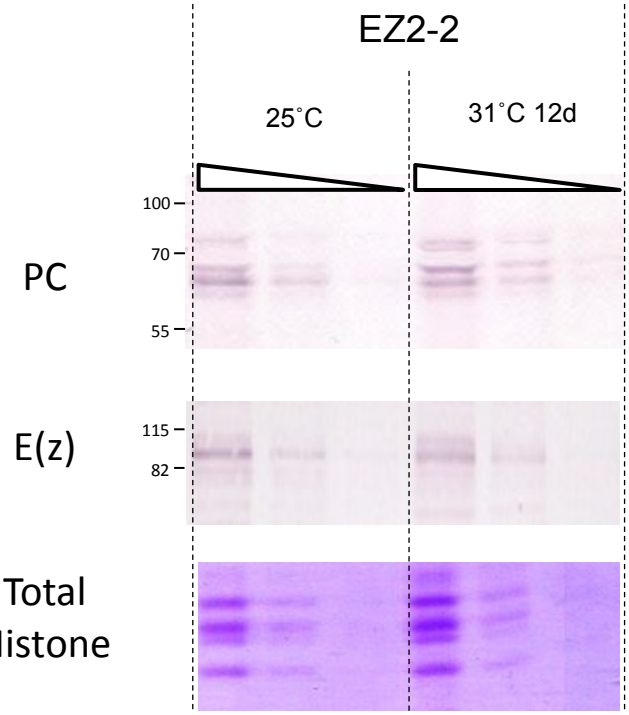

B

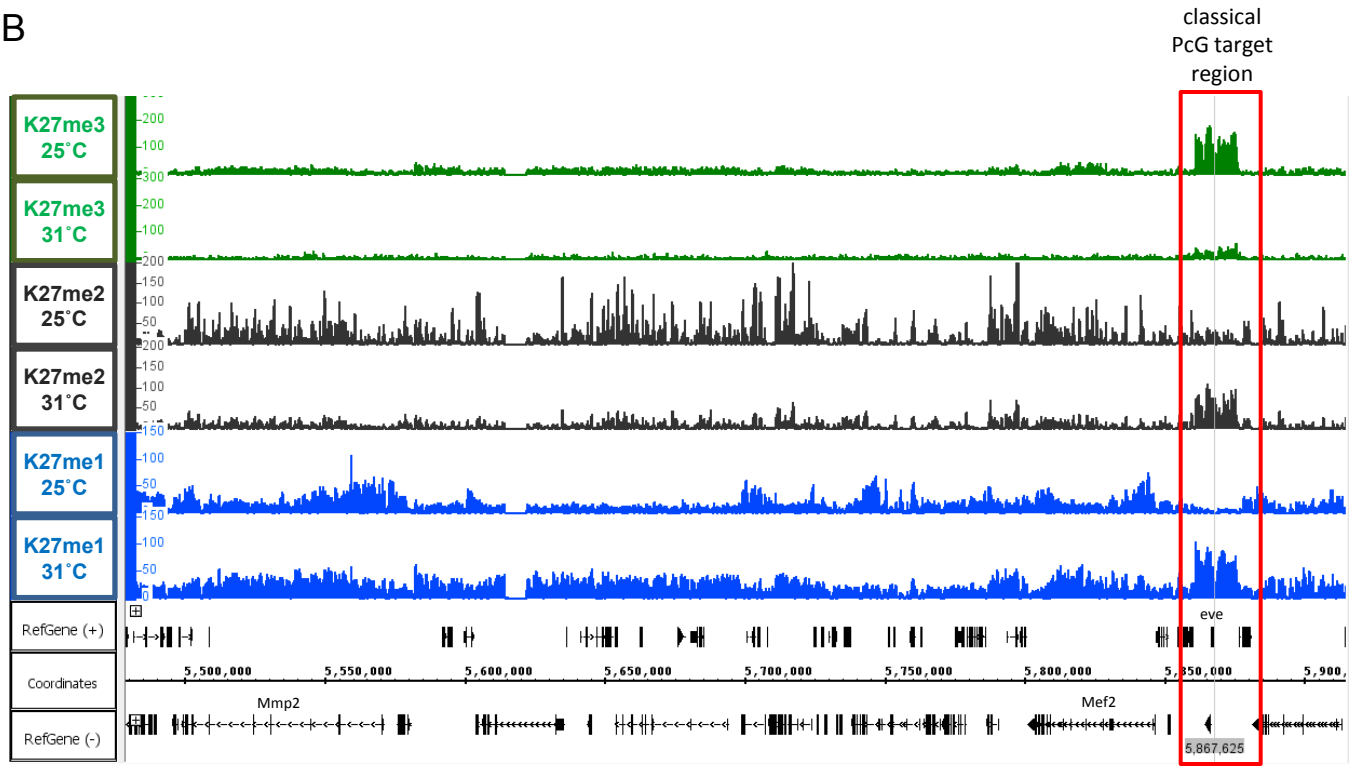

Supplemental Figure 3

A

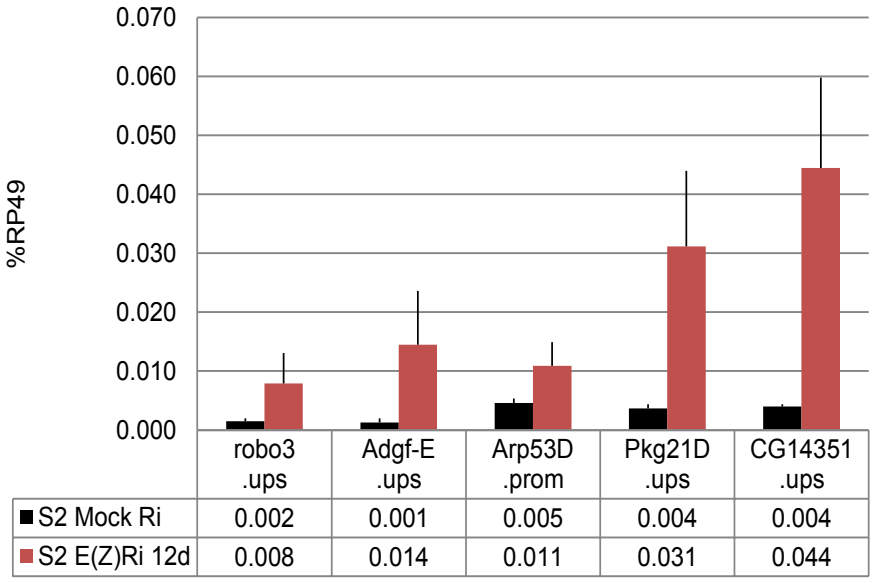

	robo3 .ups	Adgf-E .ups	Arp53D .prom	Pkg21D .ups	CG14351 .ups
S2 Mock Ri	0.002	0.001	0.005	0.004	0.004
S2 E(Z)Ri 12d	0.008	0.014	0.011	0.031	0.044

B

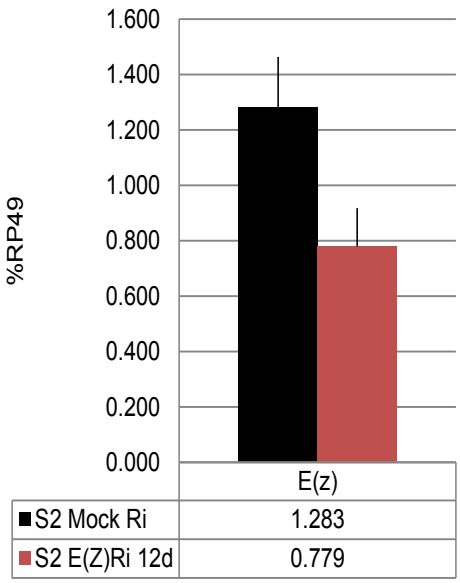

	E(z)
S2 Mock Ri	1.283
S2 E(Z)Ri 12d	0.779

C

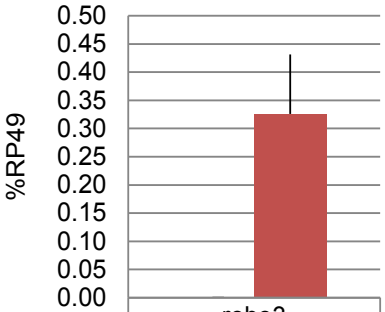

	robo3 .ups
Ras3	0.00005
SuZ12-26I3	0.32602

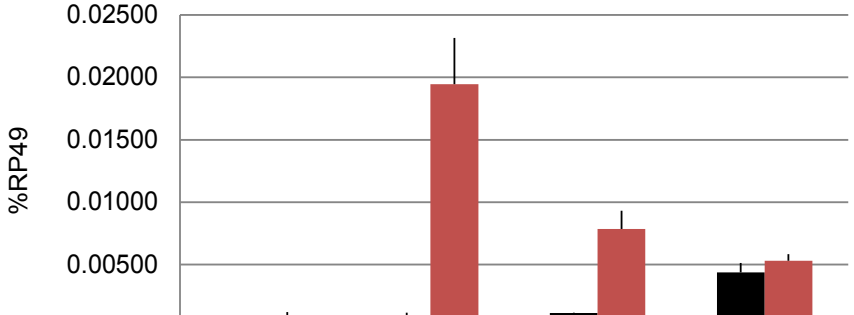

	adgf-E .ups	Pkg21D .ups	Arp53D .prom	CG14351 .ups
Ras3	0.00005	0.00073	0.00112	0.00438
SuZ12-26I3	0.00073	0.01945	0.00785	0.00531

Supplemental Figure 4

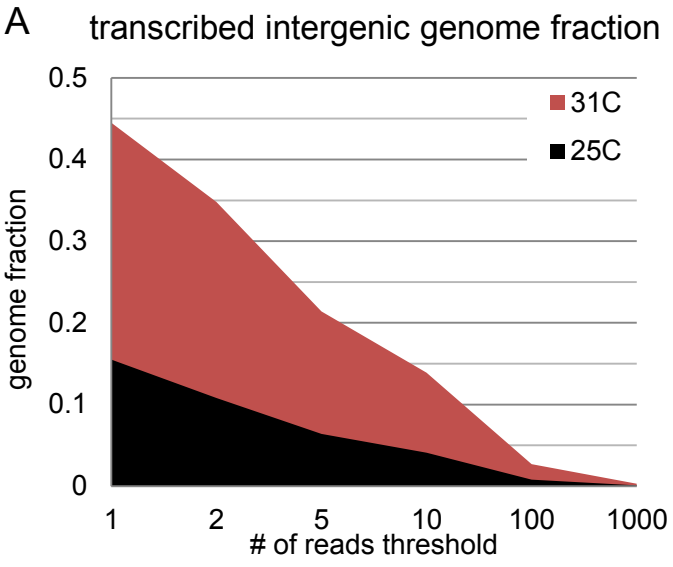

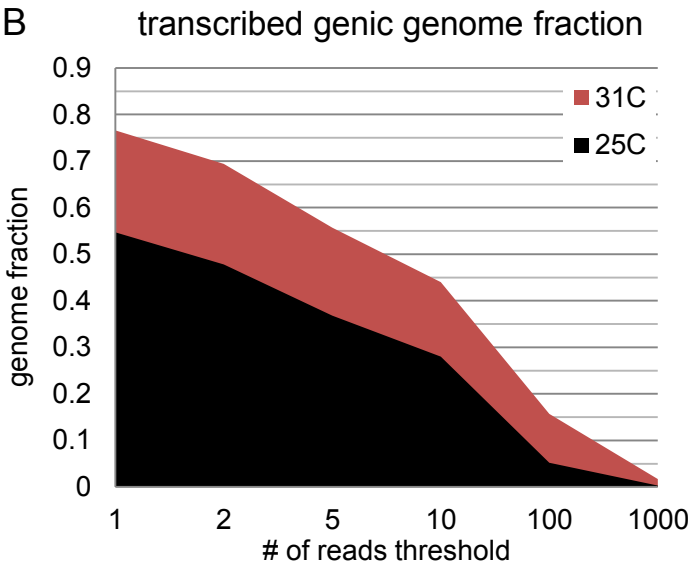

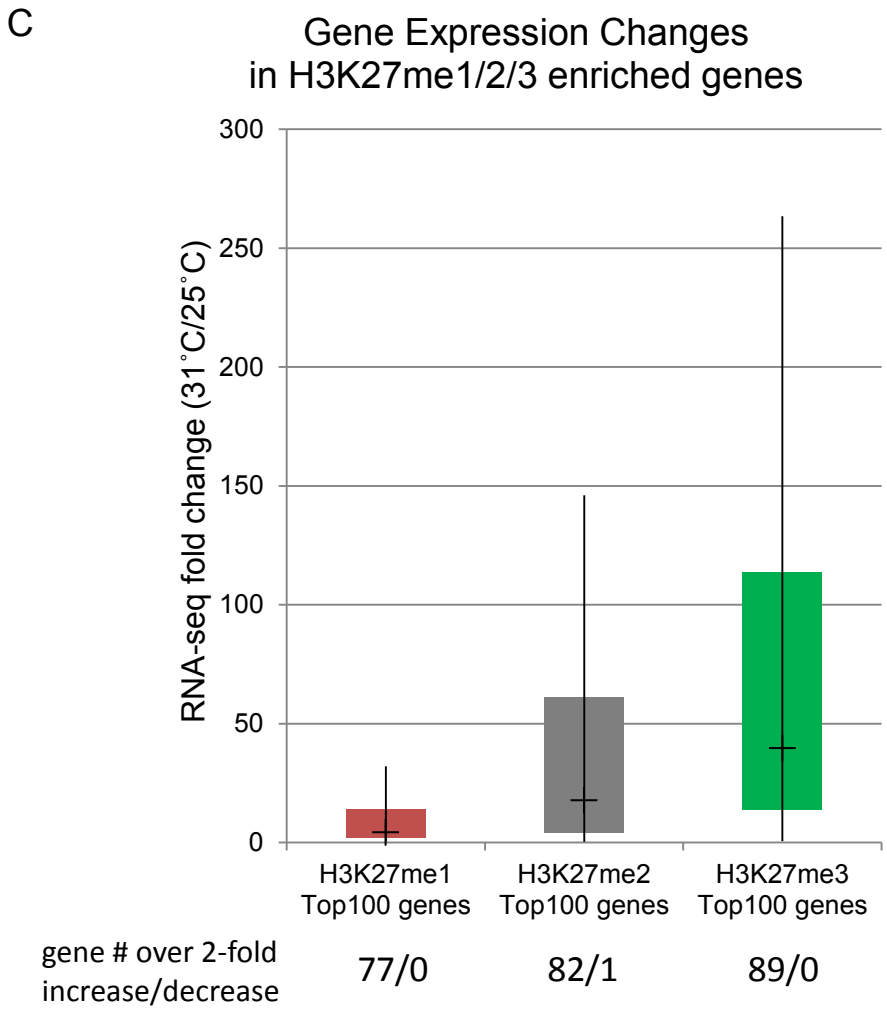

Supplemental Figure 5

A

Corr. Factors	RP49	trr	nej	brm	utx
RNAseq#1	0.263	0.206	0.330	0.345	0.555
RNAseq#2	0.209	0.396	0.162	0.274	0.341

average

RNA-seq set	qPCR-based Correction Factors (for 25C)	Standard Error
RNA-seq #1 (HG-A&B)	**0.340**	0.053
RNA-seq #2 (HG-X&Y)	**0.277**	0.038

qPCR measurement

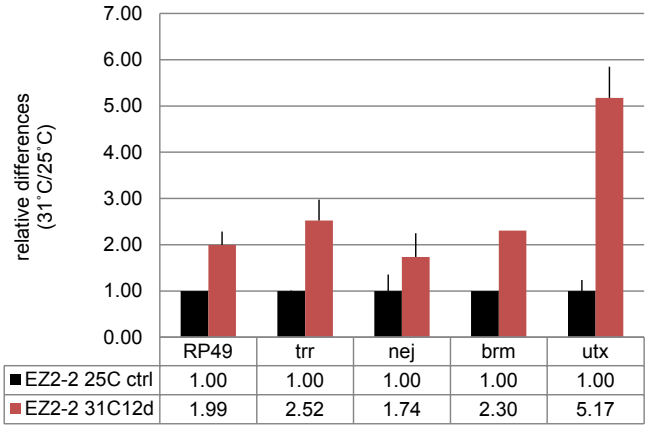

	RP49	trr	nej	brm	utx
EZ2-2 25C ctrl	1.00	1.00	1.00	1.00	1.00
EZ2-2 31C12d	1.99	2.52	1.74	2.30	5.17

RNA-seq after Normalization

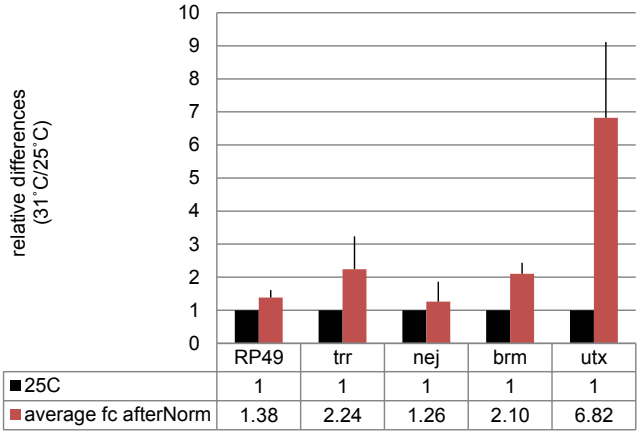

	RP49	trr	nej	brm	utx
25C	1	1	1	1	1
average fc afterNorm	1.38	2.24	1.26	2.10	6.82

B

RNA-seq Spike-in

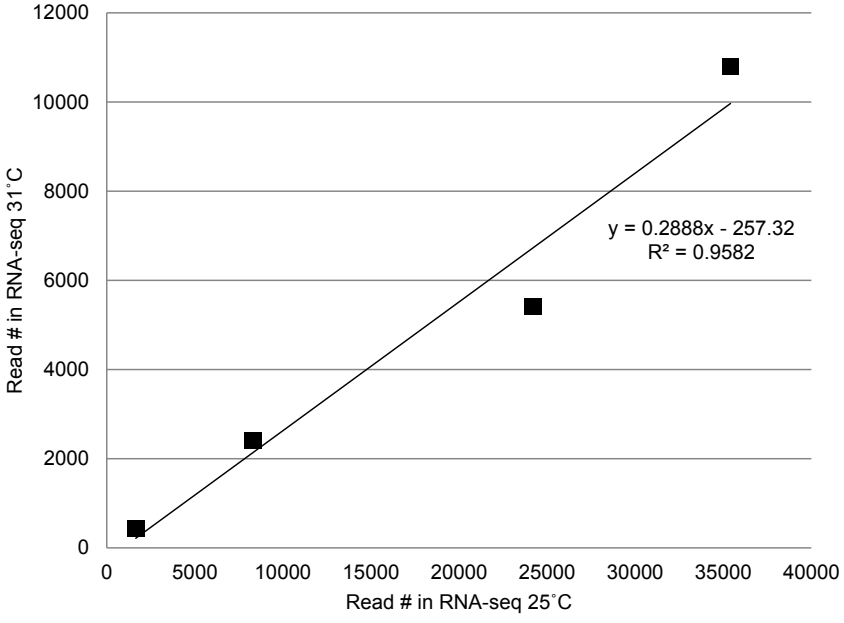

Spike-in	RNA-seq 25˚C	RNA-seq 31˚C	Corr.Factor 31˚C/25˚C
lambda.6	8294	2408	0.290
lambda.5	24194	5411	0.224
lambda.3	1646	440	0.267
lambda.4	35405	10798	0.305
total	69539	19057	**0.274**

* Correction Factor from spike-in

HG-X&Y	average	stderr
Spike in 4 pts	**0.274**	0.016

* Correction Factor from qPCR

HG-X&Y	average	stderr
qPCR 5pts	**0.277**	0.038

Supplemental Figure 6

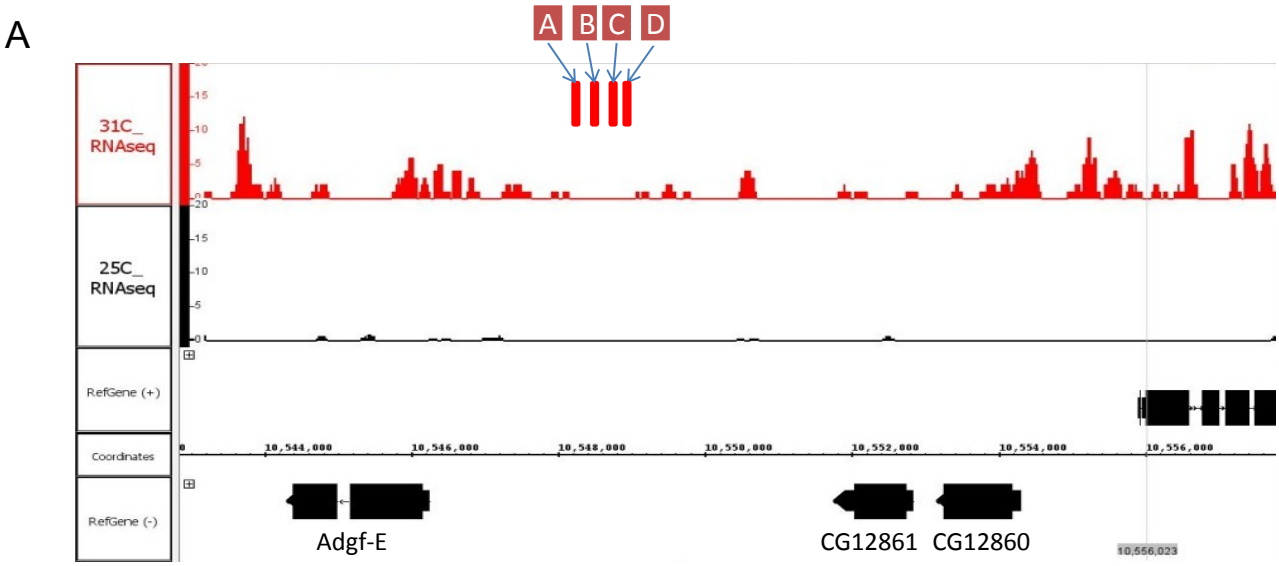

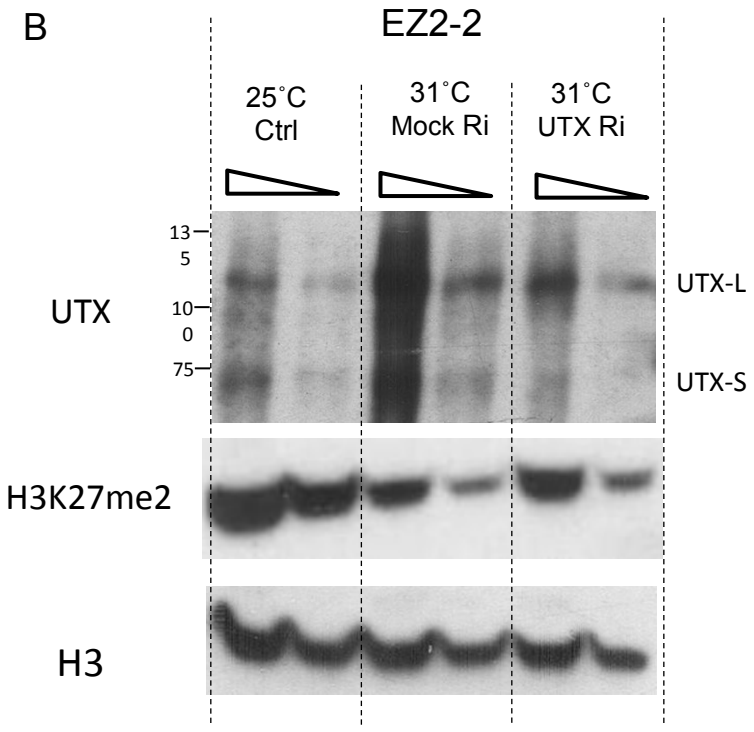

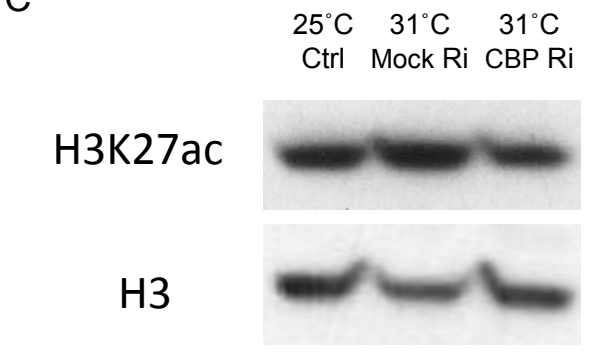

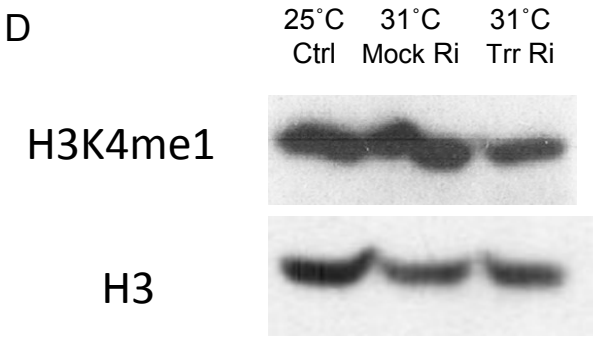

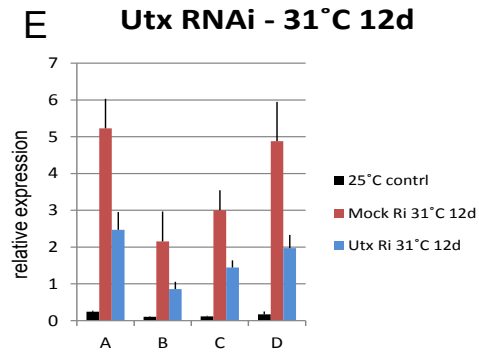

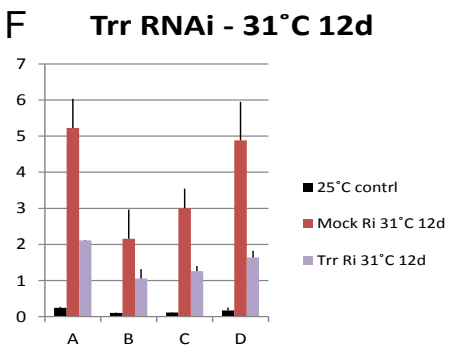

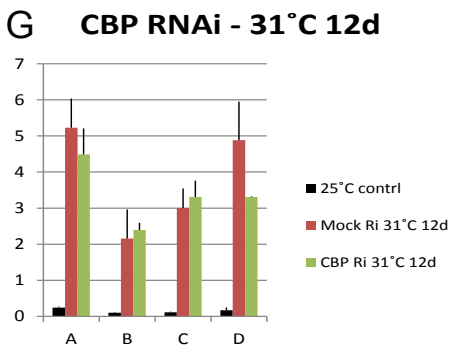

Supplemental Figure 7

A

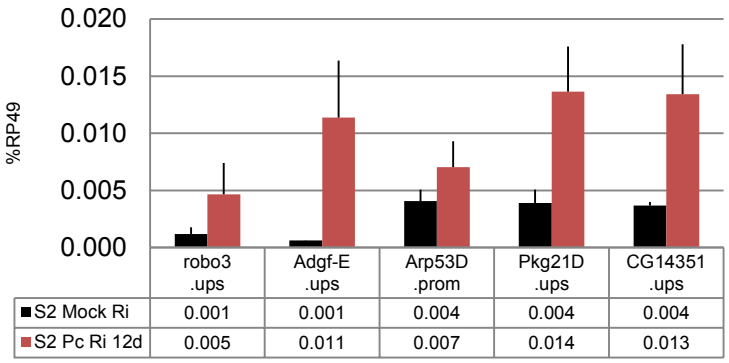

	robo3 .ups	Adgf-E .ups	Arp53D .prom	Pkg21D .ups	CG14351 .ups
S2 Mock Ri	0.001	0.001	0.004	0.004	0.004
S2 Pc Ri 12d	0.005	0.011	0.007	0.014	0.013

B

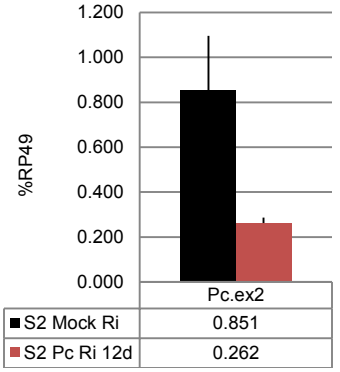

	Pc.ex2
S2 Mock Ri	0.851
S2 Pc Ri 12d	0.262

C

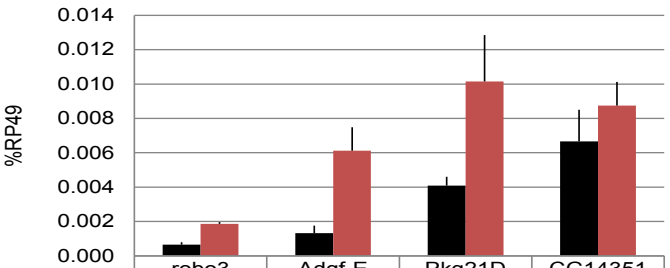

	robo3 ups	Adgf-E ups	Pkg21D ups	CG14351 ups
Mock Ri	0.001	0.001	0.004	0.007
dRingRi2	0.002	0.006	0.010	0.009

D

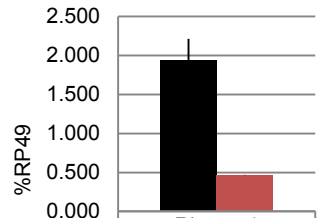

	Ring.ex1
Mock Ri	1.942
dRingRi2 13d	0.465

E

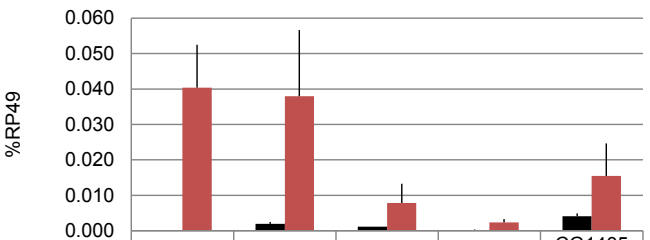

	robo3 .ups	Pkg21D .ups	Arp53D .prom	adgf-E .ups	CG14351 .ups
Ras3 (w.t.)	0.000	0.002	0.001	0.000	0.004
Pc4	0.040	0.038	0.008	0.002	0.015

G

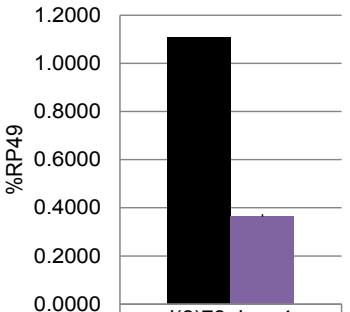

	I(3)73ah.ex4
Mock Ri	1.1061
I(3)73ah Ri	0.3633

F

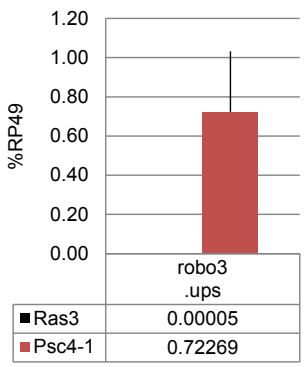

	robo3 .ups
Ras3	0.00005
Psc4-1	0.72269

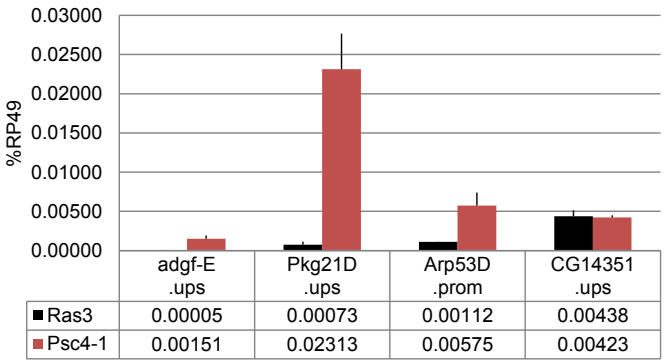

	adgf-E .ups	Pkg21D .ups	Arp53D .prom	CG14351 .ups
Ras3	0.00005	0.00073	0.00112	0.00438
Psc4-1	0.00151	0.02313	0.00575	0.00423

Supplemental Figure 8

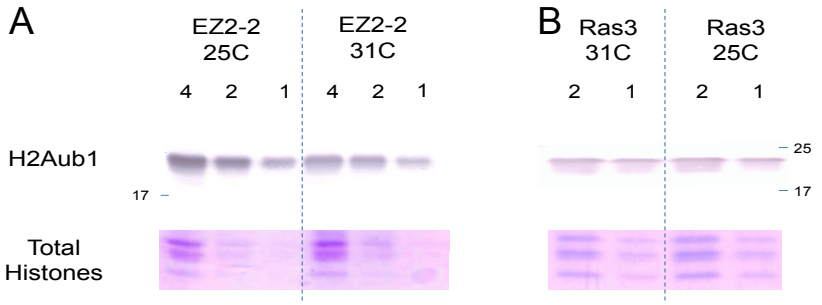

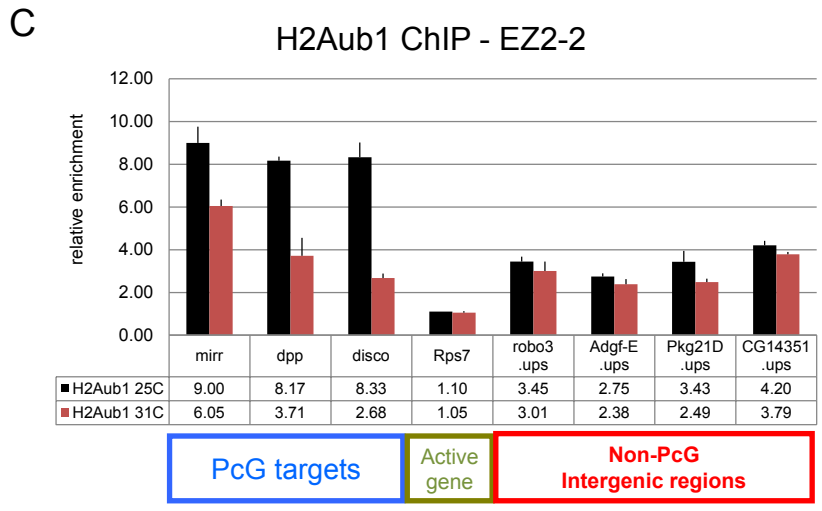

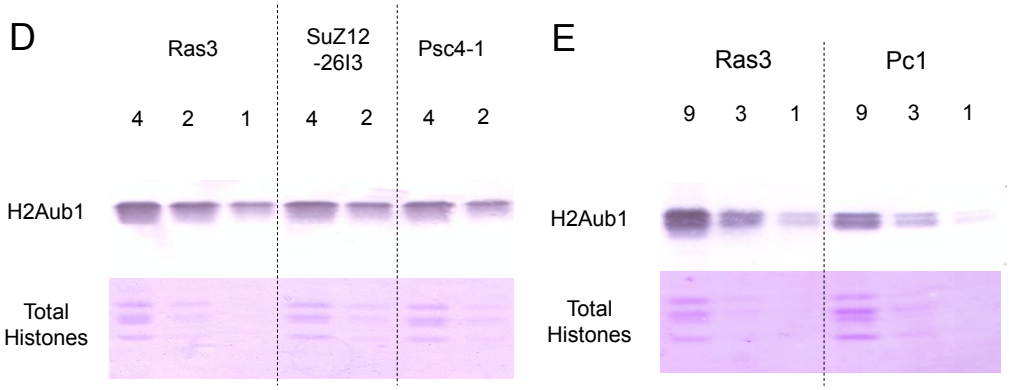

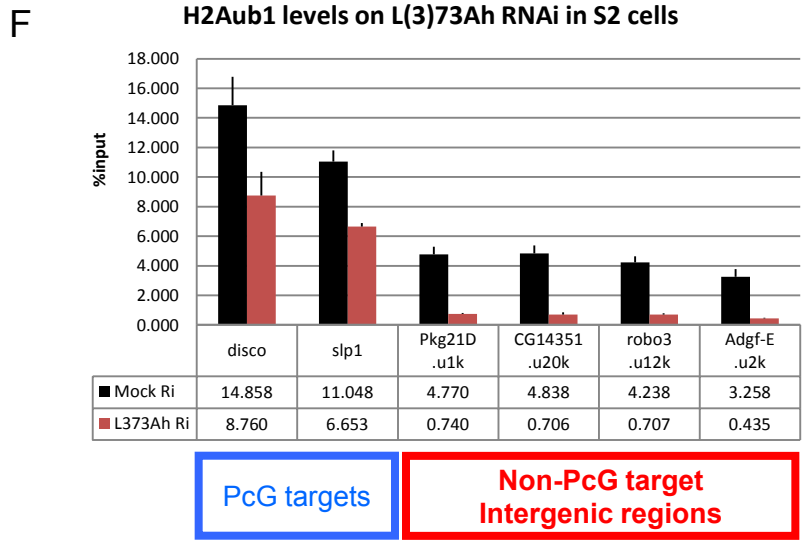

Supplemental Figure 9

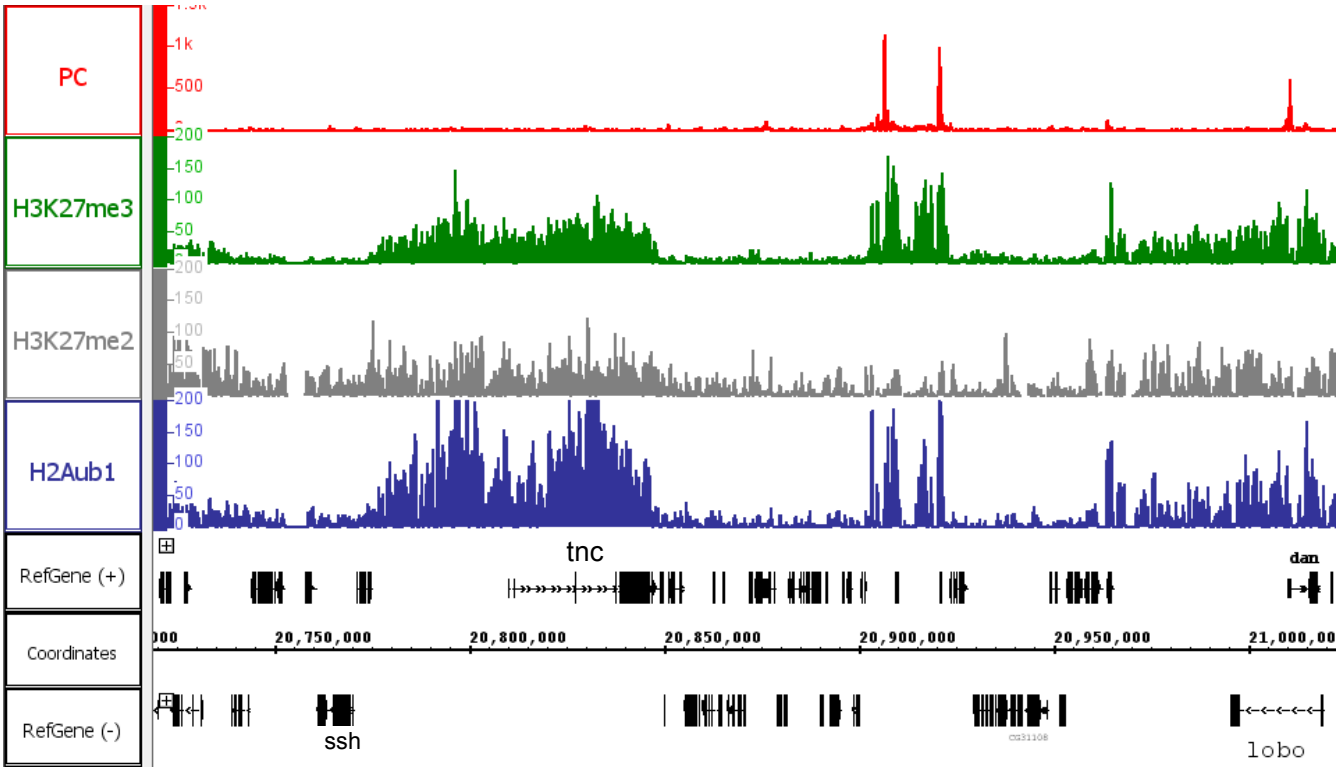

SUPPLEMENTAL METHODS

Establishment of PcG mutant cell lines

PcG mutant cell lines were established by the method of Simcox *et al*. (2008) from fly stocks carrying a transgene expressing constitutively active form of *Ras*, Ras^{V12}, to promote cell proliferation. The flies carried appropriate PcG mutations as follows: $E(z)^{61}$, also known as $E(z)^{s2}$, containing the C603Y mutation (Carrington and Jones 1996) and causing temperature sensitive 8-10-fold loss of function at 29˚C (Ketel et al. 2005); Pc^{3}, a functional null mutation not molecularly characterized; *Def(2R)Su(z)2-1.b8,* a deficiency entirely deleting the *Psc* and *Su(z)2* genes (Wu and Howe 1995); $Su(z)12^{4}$, a single nucleotide substitution resulting in translation termination and loss of functional protein (Birve et al. 2001). The resulting fly lines were crossed to generate embryos expressing Ras^{V12} and with homozygote PcG mutant background. Stable cell lines homozygous for the PcG mutations were derived from the embryos as described by Simcox *et al.* (2008). The *Su(z)2-1.b8* line was previously described by Kahn *et al.* (2014). In addition, control cell lines expressing the Ras^{V12} transgene but bearing no PcG mutation were also established.

Cell culture and RNAi

Culturing of the wild type cell lines Schneider S2, Schneider L2 Sg4, and ML-DmBG3-c2 cells was as previously described (Schwartz *et al.* 2010). The S2 cell line was obtained from Dr. Dessislava Dimova's Lab. The EZ2-2 cell line, carrying the $E(z)^{61}$ temperature sensitive mutation, grows well in firmly attached confluent monolayers at 25˚C (doubling every 3-4 days) but at 31˚C, growth become slow, cells form clumps and eventually stop growing after 4~8 days. They can still be maintained at this temperature at least 24 days if passaged without dilution. EZ2-2 cells are extremely sensitive to the cell density. Even at 25˚C, both low and high density can cause slower cell division and formation of clumps. Extensive tests were done to determine the optimal non-permissive temperature conditions for the EZ2-2 cells. The maximum temperature at which the cells can be maintained reproducibly was 31-31.5˚C.

Ras3, a wild-type control cell line generated the same way as the PcG mutant cell lines, grows well in monolayers at 25˚C and at 31˚C if the cell density is appropriately controlled but can also form clumps if overgrown.

In general, cells were splitted in every 3-4 days by optimal cell density to make initial confluency as 50-70% (e.g., 1:2 or 2:5 dilution for EZ2-2 and 1:5 to 1:10 for Ras3) in order to prevent overgrowth. For the growth curves, aliquots of the cells were collected when splitting, and relative cell number was estimated based on DNA amount from the aliquots. Each dilution factor was considered to calculate the growth rate.

The treatments with dsRNA were performed as described by Schwartz *et al.* (2010) with minor modifications. Cells were subjected to three consecutive treatments with corresponding dsRNA with growth in regular media for 4 days between each treatment. For the knock-down experiments in the EZ2-2 cell line at non-permissive temperature, one pre-treatment with dsRNA was conducted 4 days before the temperature shift.

Chromatin immunoprecipitation (ChIP) assays

ChIP was carried out essentially as described by Schwartz et al. (2006). Cells were crosslinked with formaldehyde (Sigma) to a final concentration of 1.8% for 10 min. The reaction was stopped by adding glycine to a final concentration of 0.125M on ice. The crosslinked cells were pelleted at 4˚C and washed once each with ice cold 1× PBS, and ChIP wash buffer A (10mM HEPES pH7.6; 10mM EGTA pH8.0; 0.5mM EGTA pH8.0; 0.25% Triton X-100) for 10 min, and then ChIP wash buffer B (10mM HEPES pH7.6; 200 mM NaCl; 1mM EDTA pH 8.0; 0.5mM EGTA pH 8.0; 0.01% Triton X-100) for 10min. The washed fixed cells were then pelleted, frozen in liquid nitrogen and stored in -80˚C. For use, the fixed cells were washed twice with ice cold TE buffer (10mM Tris-HCl; 1mM EDTA pH8.0) and resuspended in TE buffer with 0.1% SDS to a concentration of 1×10^8 cells/mL, and then sonicated with a Biorupter (Diagenode) set at “high” power in 5 min x 5 sessions, each with 0.5 min ON and 0.5 min OFF in ice water. After sonication, the resulting lysate was adjusted to RIPA buffer (140 mM NaCl, 10 mM Tris-HCl pH 8.0, 1 mM EDTA, 1% Triton X-100, 0.1% SDS, 0.1% sodium deoxycholate) and cleared by 5 min centrifugation at 14,000 rpm, divided in aliquots, frozen in liquid nitrogen and stored at -80˚C.

For immunoprecipitations, lysates were precleared by incubation with Protein A-Sepharose beads (Sigma). The cleared lysate was further incubated with 3-5 µg of the appropriate antibodies overnight at 4˚C. The antibody complexes were precipitated by incubation with Protein A-

Sepharose beads (Sigma or GE Healthcare) for 3 h at 4˚C. The beads were washed five times with 1 ml RIPA, once with 1 ml LiCl buffer (250 mM LiCl, 10 mM Tris-HCl pH 8.0, 1 mM EDTA, 0.5% NP-40, 0.5% sodium deoxycholate), twice with 1 ml TE (10 mM Tris-HCl pH 8.0, 1 mM EDTA). After washing, RNase A was added to a final concentration of 50µg/ml and incubated at 37˚C for 30min. To reverse crosslinking, SDS (final 0.5%), NaCl (final 140mM) and Proteinase K (final 0.5mg/ml) were added and incubated overnight at 37˚C, then transferred to 65˚C for 6hrs. The DNA was then phenol-chloroform purified, and precipitated with 100% EtOH. After incubation overnight at -20˚C, the immnunoprecipitated DNA pellet was washed with fresh 70% EtOH and dissolved either in 150µl distilled water for quantitative PCR (qPCR) analysis or in 12-50µl distilled water for ChIP-chip or ChIP-seq experiments.

Western blot analysis

Total nuclear protein was isolated by first lysing cells in hypotonic buffer containing 10% sucrose, 10mM Tris-Cl pH8.0, 10mM NaCl, 3mM $MgCl_2$, 2mM DTT , 0.2% Triton X100, 1mM PMSF and 1x Complete Protease Inhibitor (Roche) on ice, followed by centrifuging at 1500g for 3min at 4˚C and washing the nuclear pellet with Nuclear Buffer (10mM Tris-Cl pH8.0, 1mM EDTA pH8.0, 140mM NaCl, 2mM DTT, 1mM PMSF and 1x Complete Protease Inhibitor). After resuspension in Nuclear Buffer, the nuclei were lysed with Sample Buffer (12mM Tris-HCl pH6.8, 5% glycerol, 0.4% SDS, 2.9mM 2-mercaptoethanol, 0.02% bromphenol blue) by strong pipetting and boiled for 10 min. Serial dilutions of nuclear extract were loaded on SDS polyacrylamide gel, separated by electrophoresis, transferred to a PVDF membrane and detected by incubation with primary antibodies and then secondary antibodies conjugated with alkaline phosphatase or horseradish peroxidase. For the H2AK118ub antibody, the incubation buffer consisted of 5% BSA, 1x TBS, and 0.1% Tween-20.

Antibodies

Antibodies used for ChIP and western blot analysis are as follows: anti-H3K27me2 (Abcam ab24684, Diagenode pAB-046-050, or gift from Thomas Jenuwein for Sg4 ChIP-chip), anti-H3K27me3 (Abcam ab6002 for ChIP, Millipore 07-449 for western), anti-H3K27ac (Abcam ab4729), anti-H3K4me1 (Abcam ab8895), anti-H2AK118ub (Cell Signaling D27C4), anti-PC and anti-

E(Z)(both affinity purified as described by Poux et al. 2001), anti-UTX (against the entire UTX protein, affinity-purified).

RNA/DNA isolation and reverse transcription (RT)

Total RNA was isolated using the TRIzol reagent according to the manufacturer's instructions (Invitrogen). Isolated total RNA was treated with RNase-free DNase I (Roche) for 20min at 37 ˚C. DNase I was heat-inactivated by 10min incubation at 75 ˚C, and further removed by phenol extraction. DNA isolation from the same TRIzol-treated samples was performed according to the manufacturer's instructions (Invitrogen) with minor modifications. To estimate the relative cell number between multiple culture samples used for the RNA extraction, the isolated DNA was quantified by qPCR with appropriate dilution to make the Ct value between 20 and 30.

Reverse transcription was performed with 1μg of total RNA using the first strand cDNA synthesis kit with random hexamers (0.2μg per reaction) according to the manufacturer's instructions (GE healthcare). Synthesized cDNA was purified by Qiaquick PCR purification kit (Qiagen).

Quantatitive PCR and Primers

Quantitative PCRs was done to quantify RNA levels or immunoprecipitated material from ChIP assays. 2.5ul of the purified RT-PCR product or ChIP DNA (1/60 of total immunoprecipitated material) was used for each PCR reaction in a 10μl mix containing 10mM Tris-Cl pH8.3, 40mM KCl, 2.5mM MgCl2, 0.2mM dNTP, 100nM of target-specific primers, 1x EvaGreen dye (Biotium) and 1 unit of AmpliTaq Gold (Applied Biosystems). PCR was performed in 96-well plates with the Mx-3000P (Stratagene) or Realplex 2 (Eppendorf). 7-point standard curve was used for each primer pair by amplification of serial dilution of genomic DNA (four-fold dilutions for RT-qPCR) or the input DNA (two-fold dilutions for ChIP-qPCR) isolated from an aliquot of lysate that had not undergone immnunoprecipitation. Samples were appropriately diluted to be in the linear range of the standard curves. Primers were designed to amplify the regions between 100 and 200 base pairs of the target sequences. The primers are provided in Supplementary Table 1.

Overview of genome-wide distribution data

The genome-wide profiling of H3K27me2 and UTX in Sg4 cells and H3K27me3, H3K27ac, and H3K4me1 in EZ2-2 cells at permissive temperature (25˚C) and non-permissive temperature (31˚C) was performed by analysing the ChIP product with microarrays (ChIP-chip) using Affymetrix GeneChip *Drosophila* Tiling 1.0R arrays. In addition, PC, H3K27me3, Pol II ChIP-chip data from Schwartz et al. (2010) were utilized. Chromatin immunoprecipitation followed by high-throughput DNA sequencing (ChIP-seq) was performed for generating the genome-wide distribution maps of H3K27me3, H3K27me2, H3K27ac, H3K4me1, H2Aub1 and PC in EZ2-2 cells at 25˚C and 31˚C. Genome-wide ChIP-chip data for H3K27me1, H3K27me2, H3K27me3, histone H3, PC, and Pol-II in Bg3 cells were obtained from the modENCODE Project website (http://modencode.org/) (Celniker et al. 2009).

For the genome-wide transcriptional profiling of EZ2-2 cells, total RNA from EZ2-2 cells at 25˚C and 31˚C was depleted of ribosomal RNA and analysed by high-throughput RNA sequencing (RNA-seq). RNA tiling array data for the genome-wide transcriptome profiling in Bg3 cells was obtained from modENCODE Project (Celniker et al. 2009).

The *Drosophila melanogaster* genome sequence assembly Apr. 2006 (BDGP R5/UCSC dm3) was used for the analysis of the genome-wide data.

Library construction for ChIP-chip

Preparation of labeled probes for ChIP-chip was performed as described in Schwartz *et al*. (2006), with the following modifications. Briefly, one-third of the immunoprecipitated material and, in parallel, 50 ng of the ChIP input DNA were amplified using the WGA amplification kit (Sigma) following the manufacturer's instructions with a few modifications. The fragmentation step was omitted since the amplified materials are fragmented in a separated step after amplification as described later. Eighteen cycles of amplification were performed, and the resulting PCR product was purified using QIAquick PCR purification kit (QIAGEN), and 2 µg of amplified ChIP material or input DNA were fragmented to a size of 25-200 bp (peak at 75bp) by incubation with 0.5 U of DNase I (Roche) for 5-15 min at 25˚C. After heat inactivation of DNase I 10min at 95˚C, the fragmented DNA was end-labeled with bio-11-ddATP (Perkin Elmer) using recombinant Terminal Transferase (Roche). The labeled probes were hybridized to GeneChip *Drosophila* Tiling 1.0R arrays (Affymetrix) in 0.1 M MES pH 6.6, 3 M tetramethylammonium chloride (TMA), 40 pM of control oligo B2 (Affymetrix), 100 µg/ml of sonicated salmon sperm DNA and 0.02% Triton X100.

ChIP-chip data processing

The TiMAT T2 1.2.0 open source tiling microarray analysis software package was used for primary ChIP-chip data processing. The microarray results are computed in terms of the ratio between the ChIP value and the input DNA value from a control microarray. The intensity ratios between ChIP and input DNA were calculated to generate the genome-wide distribution maps. The raw intensity values were further smoothed by calculating the mean ratio over a sliding window of 675 bp along the genomic DNA sequence. Integrated Genome Browser (Affymetrix) was used for visual display of the results.

Library construction for Next Generation Sequencing (NGS)

For the RNA-seq libraries, rRNA was depleted from the 5µg of DNase I-treated total RNA by RiboZero kit (Epicentre). After purification with Agencourt RNAclean XP beads (Beckman Coulter), approximately 100-200ng of rRNA-depleted total RNA was recovered.

ChIP samples (5-10ng in 50 µl distilled water) and rRNA-depleted total RNA samples (100-200 ng in 15 µl RNase-free water) were submitted to the Rutgers University Cell and DNA Repository (RUCDR) to construct the libraries for sequencing. TruSeq ChIP Sample Preparation Kit (Illumina) was used for generating ChIP-seq libraries by following the manufacturer's instructions with a few modifications. Briefly, the size selected was 250-500bp after adaptor ligation, and the subsequent amplification was done with 15 cycles. For RNA-seq library construction, Ovation RNA-Seq System V2 kit or Encore Complete RNA-Seq Library System (NuGEN) were used. With the constructed libraries, 100bp paired-end sequencing was performed by Illumina HiSeq technology.

NGS data processing and analysis

Sequence tags from ChIP-seq libraries were mapped uniquely in the best strata of alignment to the *Drosophila* genome (FlyBase 5.22) using Bowtie v0.12.7 (Langmead et al. 2009). Sequence alignment information was further processed by SAMtools v0.1.18 (Li et al. 2009) to generate a pileup of read bases which was used for obtaining the genome-wide profiling data format (SGR format with 25bp bin) compatible with the Integrated Genome Browser (Affymetrix). RNA

sequence tags are mapped by the Genesifter pipeline (www.genesifter.net), which utilizes BWA WTS PE (GATKv3) v2 (Li and Durbin 2009) for the transcriptome alignment. Sequence tags multiply matched to repetitive sequences were excluded in all ChIP-seq and RNA-seq results.

The conventional way of normalization for the sequencing data by total number of reads (e.g., Reads Per Kilobase of transcript per Million for RNA-seq or Reads Per Million for ChIP-seq) assumes that the same amount of RNA (or immunoprecipitated DNA materials) per cell would be obtained from different samples. However, this assumption can lead to erroneous interpretations when the experiments globally affect the cell status (e.g. significantly increasing total RNA per cell or depleting more than 50% of specific histone modifications) (Lovén et al. 2012). For this reason, we normalized the NGS data based on qPCR results, which is considered to be the most reliable quantitative measurement.

Normalization of the genome-wide data from ChIP-seq or RNA-seq between different culture conditions (25˚C and 31˚C) was done by calculating the correction factors based on ChIP-qPCR or RT-qPCR results (Supplemental Figure 5, Supplemental Table S2). At least five regions were used for the normalization. For assessing the qPCR-based normalization of RNA-seq, four spike-in standards (single stranded RNA species generated from lambda DNA) were mixed to the RNA samples before library construction. The correction factors from the qPCR-based normalization and spike-in normalization were very similar (Supplemental Figure 5B). Calculated correction factors were applied to the downstream products of the NGS data analysis pipeline (e.g., SGR formatted files).

Defining PcG targets and non-PcG targets

Annotated FlyBase genes were classified as PcG targets or non-PcG targets based on the levels of PC and H3K27me3 in each cell line. All genes were sorted by maximum binding values of PC (PC_{max}) at gene bodies and 1kb flanking regions, and the genes with the PC_{max} and H3K27me3 values higher than 2 standard deviations above the mean were defined as PcG target genes. Genes with the PC_{max} values lower than the average PC_{max} value of all genes were defined as non-PcG target genes. Non-PcG target genes were further classified according to the expression level. Silent genes were defined as genes that have no detectable RNA-seq tags. The same classification was applied to the intergenic regions.

RNA-seq data for EZ2-2 cells grown at 25˚C were used to classify coding/intergenic non-PcG target regions of the EZ2-2 cells. For Bg3 cells, published modENCODE whole-genome expression data from tiling arrays were used to obtain the expression levels of coding regions.

Determining H3K27me2 enrichment

Analysis of the ChIP-chip signal distribution showed that it has two distinct bell-curved components: one from H3K27me2-enriched regions and one from low H3K27me2 regions (Supplemental Figure 1). The highest 5% point value (1.06 for Bg3, 0.99 for Sg4) from the distribution of low H3K27me2 regions was used as a threshold to determine H3K27me2 enrichment.

SUPPLEMENTAL FIGURE AND TABLE LEGENDS

Figure S1. H3K27me2 and UTX distribution in Sg4 cells

(A) The profiles of UTX, Pol II, and H3K27me2 in Sg4 cell line are shown. The BLACK chromatin regions in Kc cell line (from Filion *et al*. 2010) are shown below the H3K27me2 track.

(B) The overall distribution of H3K27me2 ChIP-chip signals was obtained by collecting the IP/input signal values from all probes on the microarray. Two hypothetical symmetric bell-curved distributions were simulated based on the overall distribution. The enrichment level of H3K27me2 was determined based on these distributions (dotted line; see Supplemental Methods).

(C) Same analysis was done for the H3K27me3 ChIP-chip as a representative of usual ChIP-chip data where only a small proportion of the genome shows enrichment.

(D-E) Meta-gene profiles of normalized levels of (D) H3K27me2 and (E) H3K27me1 by histone H3 for the PcG target genes and five sub-groups of non-PcG target genes with different expression level (e.g., NP-Q1 for the top 20 percentile actively transcribing non-PcG target genes) in Bg3 cells. RNA tiling array data from the modENCODE Project is utilized for the gene expression levels. For the numbers on x-axis represent the positions relative to transcription start sites (0.0) and transcription end sites (1.0).

Figure S2. Changes in H3K27 methylation distribution and PcG component levels after E(z) inactivation by temperature shifting

(A) The protein levels of Pc and E(z) in nuclear extracts of the EZ2-2 cells at 25°C and 31°C were determined by western blot analysis. Three-fold serial dilutions of lysate were loaded. Total histones detected by coomassie blue staining served as loading controls.

(B) The distributions of H3K27me3 (green), H3K27me2 (gray), and H3K27me1 (blue) in EZ2-2 cells at 25°C and 31°C were mapped by ChIP-seq. Merged positions of annotated transcripts from both strands are indicated in the RefSeq tracks (black).

Figure S3. Derepression in intergenic regions after *E(z)* depletion in S2 cells or *Su(z)12* mutant cells

(A-B) Expression levels in intergenic non-PcG target regions were measured by RT-qPCR analysis with total RNA from mock-treated (control; black) or *E(z)*-depleted (red) S2 cells. The expression levels are shown as relative values to those of RP49. The mRNA level of *E(z)* was monitored.

(C) Expression levels in intergenic non-PcG target regions were measured by RT-qPCR analysis with total RNA from wild type (Ras3; black) and *Su(z)12* mutant (SuZ12-26I3; red) cells.

Figure S4. Increase in the fraction of transcribing regions in the whole intergenic and genic regions of *Drosophila* genome after E(z) inactivation

(A-B) The proportion of transcribing regions in Drosophila genome (A for intergenic regions; B for genic regions) was estimated by calculating the percentage of bins (size 25bp) that have equal or more than the threshold number of reads.

(C) Gene expression level changes in the genes that are enriched by H3K27me1/2/3 (Top 100 genes) were analyzed from RNA-seq data at 25°C and 31°C. The numbers of genes that showed more than two-fold increase/decrease in transcription level are indicated at the bottom of the box plot for each histone modification.

Figure S5. Normalization of RNA-seq based on qPCR results

(A) RNA-seq data were normalized by RT-qPCR measurements on five exon regions. Correction factors for the 25°C RNA-seq data sets were calculated for all five regions by comparing the RT-qPCR results with the number of reads on RNA-seq data. Calculated correction factors were averaged and applied to the downstream products of the NGS data analysis pipeline.

(B) Four spike-in standards (1kb single stranded RNA species generated from lambda DNA) with various concentration were used to calculate a correction factor for RNA-seq data. The correction factors from the qPCR-based normalization (0.277) and spike-in normalization (0.274) were very similar to each other.

Figure S6. Knockdown effect of TrxG proteins

(A) RNA-seq tags on the Adgf-E upstream region at 25°C (black) and 31°C (red) are shown. Amplicons used for qPCR analysis in Supplemental Figures 6E-G are indicated as red bars.

(B) The protein levels of UTX and H3K27me2 levels in EZ2-2 cells at 25°C, 31°C with mock RNAi and UTX RNAi were determined by western blot analysis. Two-fold serial dilutions of lysate were loaded. Total histone H3 served as the loading control.

(C) The H3K27ac levels in EZ2-2 cells at 25°C, 31°C with mock RNAi and CBP/nej RNAi were determined by western blot analysis.

(D) The H3K4me1 levels in EZ2-2 cells at 25°C, 31°C with mock RNAi and Trr RNAi were determined by western blot analysis.

(E-G) Expression levels in Adgf-E upstream regions indicated in Supplemental Figure 6A were measured by RT-qPCR analysis with total RNA from EZ2-2 cells at 25°C and 31°C incubated with double-stranded RNA targeting LacZ (control), (E) UTX, (F) TRR or (G) CBP.

Figure S7. Intergenic expression in PRC1-deficient cells

(A-D) Expression levels in intergenic regions were measured by RT-qPCR analysis with total RNA from mock-treated (control; black) and Pc- or RING/Sce-depleted (red) S2 cells. The efficiency of the knock-down experiments was monitored by the mRNA levels of Pc and RING/Sce.

(E) Expression levels in intergenic regions were measured by RT-qPCR analysis with total RNA from wild type (Ras3; black) and *Pc* mutant (Pc4; red) cells.

(F) Expression levels in intergenic regions were measured by RT-qPCR analysis with total RNA from wild type (Ras3; black) and *Psc* mutant (Psc4-1; red) cells.

(G) The efficiency of the L(3)73Ah knock-down experiments was monitored by the mRNA level of *l(3)73Ah*. See Fig.6F for the expression levels in intergenic and exon regions in mock-treated and L(3)73Ah-depleted S2 cells.

Figure S8. Changes in H2Aub1 levels after E(z) inactivation and in PcG mutant cell lines

(A-B) The global H2AK118ub1 levels in nuclear extracts of the EZ2-2 cells and Ras3 wild type cells at 25℃ and 31℃ were determined by western blot analysis. Two-fold serial dilutions of lysate were loaded. Total histones detected by coomassie blue staining served as loading controls.

(C) The H2AK118ub1 levels of PcG and non-PcG target regions in EZ2-2 cells at 25℃ and 31℃ were measured by ChIP-qPCR.

(D) The global H2AK118ub1 level of the Ras3 (w.t.) cells is compared with *Psc* and *Su(z)12* mutant cells. Two-fold serial dilutions of lysates were loaded. Total histones detected by coomassie blue staining served as loading controls.

(E) The global H2AK118ub1 level of the Ras3 (w.t.) cells is compared with Pc mutant cells. Three-fold serial dilutions of lysate were loaded. Total histones detected by coomassie blue staining served as loading controls.

(F) The H2AK118ub1 levels at PcG and non-PcG target regions after L(3)73Ah knock-down in S2 cells were measured by ChIP-qPCR.

Figure S9. H2Aub1 distribution in PcG and intergenic non-PcG target regions

The distributions of PC (red), H3K27me3 (green), H3K27me2 (gray), and H2Aub1 (dark blue) in EZ2-2 cells at permissive temperature were mapped by ChIP-seq. Merged positions of annotated transcripts from both strands are indicated in the RefSeq tracks (black).

Table S1. List of primer sequences

amplicon names	Forward primer	Reverse primer	class	location information
robo3.ups.12k.B	AAATTGCACACCCCAGCATC	TCGAGGGGCGGAACTAATTT	non-coding region	robo3 12kb upstr.
Adgf-E.ups.B	GTCAAAACCCTGGCGATAAG	CCTGGGGGTCTATTGTCTCA	nc region	Adgf-E 2.5kb upstr.; D in Fig. S6A
Pkg21D.ups1k.A	AATCCTGCAGAGCCAGCTAA	CTCATCCCCTTCCACTTTCA	nc region	Pkg21D 1kb upstr.
Arp53D.prom.1	CGATTTTTGGCCTCTGTATGT	GCTGTGTTCCAGTCGGATTT	nc region	Arp53D 200bp upstr.
CG3837.prom.A	GAATCGAATGCCATCAGTCC	CGCTTGAATGTCAATGTCGT	nc region	CG3837 promoter
inaC.ups.B	GCCTTGCCAGCCAGCGTGTCCT	AGCGCCGCCCCTGCAAGCCA	nc region	inaC 1.3kb upstr
CG14351.ups.20k.B	ACTCCTCTGCTTCCCCCACT	ATGCTTGGATGGTTGGATGG	nc region	CG14351 20kb upstr
n-syb.dns.A	AGGGGCCATCGATTCCTTT	CCAGGCGCCTATTTACCACA	non-coding region	n-syb downstr.
robo3.12k.C	ATAGTTGGCGAAGCAGTCGT	CCACACTCGGCTTTGATCTT	nc region	robo3 12kb upstr.
robo3.u9k.A	TAATGCCCGACTGCTCTGTTG	ACTTGCATGCAGCACTCACAC	nc region	robo3 9kb upstream
robo3.u10k.A	CACCATCTGCCTGCGTTTATC	ACCCGGCAAACACATATACCC	nc region	robo3 10kb upstr.
adgf-E.ups2K.3n4	GCTTCATTATCCGGGCCAAC	CATTATTTTGTTGCGGTGGTCT	nc region	Adgf-E upstr.; A in Fig. S6A
adgf-E.ups2k.5n6	TGGCTTGTGAAGATTAAACGAA	GGGAAACATTTAGGAAGATCTGG	nc region	Adgf-E upstr.; B in Fig. S6A
adgf-E.ups2k.7n8	GCATAAACACAAGCGTTGAATGT	TACATTTGTCGTCGGCTGCAC	non-coding region	Adgf-E upstr.; C in Fig. S6A
abd-b.tx5	ATTCGACTGGGAGTGTTTCG	GCGACACGATGTTTTGATTG	PcG target	Abd-B exon
slp1.ex1.B	GGAGGTATTCATTGGCGAGA	GTATGGTGAAGCAGCCATCA	PcG target	slp1 exon
disco.ex1.B	GTGCATAAGTGTGCGTGCAT	ACTGTTGGAGCTGTGTGCTG	PcG target	disco exon
Dr.ex1.B	TGTGTCTGTGTTTCCCAAGC	GCCGGTTAATTGGTTCATTG	PcG target	Dr exon
dpp.tx3	TCTCGGACCCCCATATACAA	AACCCGTCAGTTGACATTCC	PcG target	dpp exon

mirr.ex2	ATACGGGTCGCACCATCTAC	ACATGCCCTCCGGATAGAC	PcG target	mirr exon
U-ex1	GTCTTTGTAGCCATTCACCG	CCCTATGCCAACCACCATC	PcG target	Ubx exon
Antp-ex1	TAATTTTGTGCTTTGGGATT	GAACATAGGAACAGGAACCA	PcG target	Antp exon
RP49	GAAGAAGCGCACCAAGGACT	AACGCGGTTCTGCATGAGCA	coding-region	RP49(Rpl32) exon
CG30480.ex1	CTTATCAACCTCCCCAGCAA	TTGGGGTGCATATCCATTTT	coding-region	CG30480
Arp53D.ex	GGATTCCGTGATCGGTGATA	CTGCCAAACCATCTCCATTT	coding-region	Arp53D exon
ind-ex1	ACCTGGAAGCTTCTGCACAT	ACCTCCCGAAGAGTGGTTCT	coding-region	ind exon
CG3837.ex7	ATCGCCTGAATAGCGAGAAG	ACGCATTTTTCCTCCACTTG	coding-region	CG3837 exon
Pc-ex2	GCCGTAACTAAAACTAGCCA	CGAGCCCATAGACTCATTAC	coding-region	Pc exon
EZEX2	CCGTGGCAAGGTTTACGAC	CGTATCTGTAGTCAAAGAATAG	coding-region	E(z) exon
dRingEx1	CATTTTCACACCAATTCTGA	CGGTCACACTTCAAGCTAAT	coding-region	RING/Sce exon
dUTX.ex4	GAAGCTGACCCAAAGAGTGG	CCGAGTTGCGATATGCTAGG	coding-region	dUTX exon
trr-ex1	CGCAAGACACAGCAGATGG	CTTGTCCTCGATGATCTTGC	coding-region	trr exon region
nej.ex6	GCGGCGTGTGTATATTGCCTA	TGGGATGGCAGTGAAAGATGT	coding-region	nej exon
l-3-73ah.ex4	GGGTCGAGCTCTAACCACTGT	GGTTTCGAGGGGACTAACACT	coding-region	l(3)73ah exon
brm.ex3	AACTCACCCAGGTGCTGAACA	CGAGGGCAGCAGGAAATTAAG	coding-region	brm exon
bxdPRE	GCCATAACGGCAGAACCAAAG	ATGAGGCCATCTCAGTCGC	PcG target	bxd PRE
Antp-1	AAGCCCAGCCCACTTAGCCT	CAGCTGTCGAGGTGTGTGGC	PcG target	Antp PRE
dpp.PRE2	GCAACAGGCAATGCAATCTA	AACTCGGGGCTCTTTCTTTC	PcG target	dpp PRE
pr-slp	CTTCGTGTAGACTTCGTTCG	GATTCTCACACACGACTTGG	PcG target	slp1 PRE
mirr.PRE1	TAATCGCTTGCACTCGACAC	TCCGTTTCAGCTTTCGACTT	PcG target	mirr PRE
Mcp-chip	ATAAGGGCTTTTCTGGGGAAG	TGTAAGGAGGAAGACTACATC	PcG target	MCP PRE
w-pr	CTGCACTGGATATCATTGAAC	GCGAGAGGAGTTTTGGCAC	ChIP negative control	white promoter
Rps7-ex3	GACTCTGACCGCTGTGTACG	GGTGGTCTGCTGGTTCTTGT	ChIP negative control	Rps7 exon
UTXRNAI	CTAATACGACTCACTATAGGGAG TATCCGCATAGCCAACTCAG	CTAATACGACTCACTATAGGGAG TGGCTATGGTTGTGTGAGAC	dsRNA primers	dUTX RNAi; cDNA template

trr-Ri1	CTAATACGACTCACTATAGGGAGA GCAAAGCGGTGGTCAGCA	CTAATACGACTCACTATAGGGAGG GAGCCAGACTAACGCTGAG	dsRNA primers	Trr-RNAi
nej-Ri1	CTAATACGACTCACTATAGGGAGC AGCATTGTGCCTCTTCGC	CTAATACGACTCACTATAGGGAGC ATCAGGACACTGGAACCG	dsRNA primers	CBP-RNAi
EZRi1	CTAATACGACTCACTATAGGGAG TACAGGATCTGTACTGCGAG	CTAATACGACTCACTATAGGGAG GCTTGTCCTTGACTTCTTCC	dsRNA primers	E(Z) RNAi.1
EZRi2	CTAATACGACTCACTATAGGGAG CTGGCATGATGAACATCACC	CTAATACGACTCACTATAGGGAG TTGGGATATGATCTCGCCAC	dsRNA primers	E(Z) RNAi.2; cDNA template
LZRi1	CTAATACGACTCACTATAGGGAG GGCCACCGATATTATTTGCC	CTAATACGACTCACTATAGGGAG CACACTGAGGTTTTCCGC	dsRNA primers	LacZ RNAi
dRing.Ri2	CTAATACGACTCACTATAGGGAG AGGGTGACTCCAACATCGAC	CTAATACGACTCACTATAGGGAG GTCTGGTTGCCATTCAGGAT	dsRNA primers	RING/Sce RNAi
PCRi1	CTAATACGACTCACTATAGGGAG AGTACCGTGTCAAGTGGAAG	CTAATACGACTCACTATAGGGAG TTTGGTATGTTATTGTTCTCGG	dsRNA primers	PC RNAi
l-3-73ah.ex1.Ri1	CTAATACGACTCACTATAGGGAG AACAAATCGCGACCAAAATC	CTAATACGACTCACTATAGGGAG GTGGTGGCATCGATGAAGTAG	dsRNA primers	l-3-73ah RNAi.1
l-3-73ah.ex3.Ri2	CTAATACGACTCACTATAGGGAG GACAACGAGAAGGTGATGGAC	CTAATACGACTCACTATAGGGAG GTACTTTTCGATGCCGTTGAG	dsRNA primers	l-3-73ah RNAi.2
lambda-3	CTAATACGACTCACTATAGGGAG TCCAAAGTTCTCAATGCTGCT	TTACGGTTGATTTCGAGTTGG	ssRNA for spike-in	lambda
lambda-4	CTAATACGACTCACTATAGGGAG GCATTGCAGCAGATTAAGGAG	CAAAAAGCATCGGGAATAACA	ssRNA for spike-in	lambda
lambda-5	CTAATACGACTCACTATAGGGAG CTTGAGGGTGAATGCGAATAA	TGAACTGAAATGCCCGTTTAC	ssRNA for spike-in	lambda
lambda-6	CTAATACGACTCACTATAGGGAG CGGTTGTAAGTTCCGCAATAA	GCGACTCTGGGAACAATATGA	ssRNA for spike-in	lambda

Table S2. Correction factors for the ChIP-seq data sets

ChIP-seq set	qPCR-based Correction Factors (for 31C)	SEM of qPCR-based CF
H2Aub1 #1 (HG09&10)	1.043	0.032
H2Aub1 #2 (HG27&28)	0.843	0.063
H3K27me3 #1 (HG29&30)	0.237	0.053
H3K27me3 #2 (HG151&152)	0.336	0.090
H3K27me2 #1 (HG25&26)	0.405	0.043
H3K27me2 #2 (HG149&150)	0.190	0.040
H3K27ac #1 (HG31&32)	1.677	0.224
H3K27ac #2 (HG153&154)	1.366	0.130
H3K4me1 #1 (HG33&34)	1.057	0.047
H3K4me1 #2 (HG155&156)	1.426	0.190

Table S1. List of primer sequences

Detailed information of the primer pairs used in this study is described.

Table S2. Correction factors for the ChIP-seq data sets

Correction factors for the ChIP-seq data sets were calculated based on ChIP-qPCR measurements similar to the way for RNA-seq normalization.

Supplemental References

Birve A, Sengupta AK, Beuchle D, Larsson J, Kennison JA, Rasmuson-Lestander A, Müller J. 2001. Su(z)12, a novel Drosophila Polycomb group gene that is conserved in vertebrates and plants. *Development* **128**: 3371–9.

Carrington E, Jones R. 1996. The Drosophila Enhancer of zeste gene encodes a chromosomal protein: examination of wild-type and mutant protein distribution. Development 122: 4073–4083.

Celniker SE, Dillon LAL, Gerstein MB, Gunsalus KC, Henikoff S, Karpen GH, Kellis M, Lai EC, Lieb JD, MacAlpine DM, et al. 2009. Unlocking the secrets of the genome. *Nature* **459**: 927–30.

Clemens JC, Worby CA, Simonson-Leff N, Muda M, Maehama T, Hemmings BA, Dixon JE. 2000. Use of double-stranded RNA interference in Drosophila cell lines to dissect signal transduction pathways. *Proc Natl Acad Sci U S A* **97**: 6499–503.

Ketel CS, Andersen EF, Vargas ML, Suh J, Strome S, Simon JA. 2005. Subunit contributions to histone methyltransferase activities of fly and worm polycomb group complexes. *Mol Cell Biol* **25**: 6857–68.

Langmead B, Trapnell C, Pop M, Salzberg SL. 2009. Ultrafast and memory-efficient alignment of short DNA sequences to the human genome. *Genome Biol* **10**: R25.

Li H, Durbin R. 2009. Fast and accurate short read alignment with Burrows-Wheeler transform. *Bioinformatics* **25**: 1754–60.

Li H, Handsaker B, Wysoker A, Fennell T, Ruan J, Homer N, Marth G, Abecasis G, Durbin R. 2009. The Sequence Alignment/Map format and SAMtools. *Bioinformatics* **25**: 2078–9.

Lovén J, Orlando DA, Sigova AA, Lin CY, Rahl PB, Burge CB, Levens DL, Lee TI, Young RA. 2012. Revisiting Global Gene Expression Analysis. *Cell* **151**: 476–482.

Simcox A, Mitra S, Truesdell S, Paul L, Chen T, Butchar JP, Justiniano S. 2008. Efficient genetic method for establishing Drosophila cell lines unlocks the potential to create lines of specific genotypes. ed. R.S. Hawley. *PLoS Genet* **4**: e1000142.

Wu C-T, Howe M. 1995. A genetic analysis of the Suppressor 2 of zeste complex of Drosophila melanogaster. Genetics 140: 139–181.